CARBON 77 (2014) 538–550

Available at www.sciencedirect.com

ScienceDirect

journal homepage: www.elsevier.com/locate/carbon

Thermal and electrical conduction in the compaction direction of exfoliated graphite and their relation to the structure

Po-Hsiu Chen, D.D.L. Chung *

Composite Materials Research Laboratory, University at Buffalo, State University of New York, Buffalo, NY 14260-4400, USA

ARTICLE INFO

Article history:
Received 1 February 2014
Accepted 24 May 2014
Available online 5 June 2014

ABSTRACT

The effects of the compaction and graphite layer preferred orientation on the thermal and electrical conductions in the compaction direction of graphite-flake-based exfoliated graphite have been decoupled. The compact's electrical and thermal conductivities decrease with increasing compaction (density increasing from 0.047 to 0.67 g/cm^3, solid content increasing from 2.1 to 30 vol.%) and preferred orientation. The essentially linear correlation between electrical and thermal conductivities (Wiedemann–Franz Law) is because both conductions are governed by the preferred orientation. With increasing compaction, the fraction (f) of conduction path that is the graphite a-axis decreases from 0.997 to 0.937 and from 0.994 to 0.798 for thermal and electrical conductions respectively. For the solid-part thermal and electrical conductivities to exceed 140 W/(m K) and 60 kS/m respectively, f must exceed 0.95; the highest solid-part conductivities are 550 W/(m K) and 230 kS/m. The compaction-related variation in the solid-part conductivities is large [21–550 W/(m K) and 10–230 kS/m], due to the preferred orientation variation. The through-thickness Lorentz number (7.3×10^{-6} W Ω/K^2) is similar to the in-plane value, being independent of the preferred orientation. At 2–7 vol.% solid, conductivities of 7 W/(m K) and 3 kS/m are obtained for the compact – toward the targets for fuel cell biopolar plates.

1. Introduction

Exfoliated graphite is elongated graphite particles obtained by the exfoliation (typically involving rapid heating) of intercalated graphite flakes [1–3]. During exfoliation, expansion typically by hundreds of times occurs along the c-axis of the graphite, thus causing the elongation. Due to the cellular structure of exfoliated graphite, the particles of exfoliated graphite mechanically interlock onto one another upon compaction [4], thereby forming a continuous flexible sheet (known as "flexible graphite" [5,6]) in the absence of a binder, such that the plane of the sheet is perpendicular to the direction of compaction and the graphite layers exhibit preferred orientation in the plane of the sheet [4,7,8]. Due to the preferred orientation, the thermal conductivity is much higher in the plane of the sheet than the through-thickness direction [9].

Flexible graphite is all graphite, so it is similar to conventional graphite in terms of the high-temperature resistance, low coefficient of thermal expansion and excellent corrosion resistance. It is used for gaskets for harsh environments, such

* *Corresponding author:* Fax: +1 (716) 645 2883.
E-mail address: ddlchung@buffalo.edu (D.D.L. Chung).
URL: http://www.alum.mit.edu/www/ddlchung (D.D.L. Chung).
http://dx.doi.org/10.1016/j.carbon.2014.05.059
0008-6223/

as acid and high temperature environments. Due to the low cost of graphite flakes, flexible graphite is inexpensive compared to conventional monolithic graphite, the fabrication of which requires high temperatures. For example, the fabrication of carbon foam of high thermal conductivity requires carbonization at 1050 °C, followed by graphitization at >2400 °C [10]. The ease of shaping is another advantage of flexible graphite. For example, grooves can be formed in a flexible graphite sheet during sheet fabrication by compaction of the exfoliated graphite using an appropriately grooved piston, so that machining is not needed. In case of conventional monolithic graphite, expensive machining is necessary, due to the brittleness of graphite [11].

Prior work has shown that an increase in the compacting pressure causes decrease in the through-thickness thermal conductivity [9,12], increase in the in-plane thermal conductivity [12,13] and increase in the in-plane electrical conductivity [4,9]. Since an increase in compaction pressure increases both the density and the degree of preferred orientation of the graphite layers perpendicular to the compaction direction, the decoupling of these two contributions to the effect of the compacting pressure is needed for basic scientific understanding of the structure and properties of the solid part of the exfoliated graphite compact. Through modeling, this decoupling has been performed in relation to the electrical conductivity for exfoliated graphite compacts that are isotropic and very low in density (at solid contents around the percolation threshold) [4]. Percolation is necessary for mechanical interlocking to occur between the worms and the interlocking is important for the mechanical integrity of the compact. Therefore, solid contents that are beyond the percolation threshold are practically important. In relation to the thermal conductivity for exfoliated graphite compacts that are anisotropic, the decoupling has been performed partially, as it yields the thermal conductivity anisotropy of the solid part of the compact, but not the thermal conductivity of the solid part [12]. The first objective of this paper is to provide this decoupling (through modeling that utilizes measured values) for both the thermal and electrical conductivities in the through-thickness direction for exfoliated graphite compacts at solid contents that are beyond the percolation threshold, thereby obtaining new information on the structure and electrical/thermal conduction behavior of technologically relevant exfoliated graphite compacts.

Prior work has shown that an increase in the compaction pressure increases the thermal conductivity anisotropy of the solid part of the exfoliated graphite compact, such that the anisotropy is up to 80 at a density of 1.4 g/cm^3 [12]. It was assumed that the contribution of the *a*-axis path to the through-thickness thermal conductivity ranges from 0.5 to 1 as the density is increased [12]. However, the extent of contribution of the *a*-axis conduction path vs. that of the *c*-axis conduction path to the thermal conduction has not been determined. The second objective of this work is to determine the relative contributions of the *a*-axis and *c*-axis conduction paths in the through-thickness thermal conduction of exfoliated graphite compacts.

The expected positive correlation of the in-plane thermal and electrical conductivities of flexible graphite has been previously reported, though the correlation plot reported was for the thermal conductivity vs. the electrical resistivity (rather than the electrical conductivity) and the shape of this plot was interpreted to mean that the Wiedemann–Franz law was not obeyed [9]. On the other hand, calculation based on the data in this plot, as performed in the present work, shows that the Lorentz number ranges from 5.6×10^{-6} W Ω/K^2 at a low compaction pressure to 6.2×10^{-6} W Ω/K^2 at a high compaction pressure. The small variation of the Lorentz number in this range suggests that the Wiedemann–Franz law is at least approximately obeyed for the in-plane thermal and electrical conductivities. At any rate, the scientific origin of the correlation has not been elucidated in prior work [9]. Moreover, the correlation of the through-thickness thermal and electrical conductivities of flexible graphite or exfoliated graphite compacts has not been previously reported. The third objective of this paper is to determine and elucidate this correlation for the through-thickness direction, thereby determining the through-thickness Lorentz number, shedding light on the through-thickness conduction mechanism, and facilitating the tailoring of the through-thickness thermal and electrical conductivities.

Corrosion resistant, low hydrogen-gas permeability, low thermal expansion, chemically resistant (resistant to fuel, oxidant, water and acidic conditions) and high-temperature resistant sheets that are thermally and electrically conductive in the through-thickness direction are needed for the bipolar plates of fuel cells [14] and flow batteries [15]. Flexible graphite is attractive for its corrosion resistance, low gas permeability, low thermal expansion, chemical resistance and high-temperature resistance. Grooves are needed in a bipolar plate for the purpose of directing the flow of the gas that is involved in the electrochemical reaction. Flexible graphite is also attractive for the bipolar plates due to their shapeability. However, the electrical and thermal conductivities of flexible graphite are inadequate in the through-thickness direction, which is the relevant direction for bipolar plates. The electrical conductivity needs to exceed 100 kS/m (industrial target), while the thermal conductivity needs to exceed 10 W/(m K) (industrial target) [11]. This shortcoming of flexible graphite is due to the preferred orientation of the graphite layers in the plane of the sheet. The fourth objective of this paper is to enhance the electrical and thermal conductivities in the through-thickness direction by decreasing the compaction pressure during the fabrication of the sheet. The decrease in the compaction pressure is expected to increase undesirably the hydrogen-gas permeability and increase desirably the shapeability, but these effects are outside the scope of this paper.

It has been reported that the through-thickness thermal conductivity increases with decreasing density (decreasing compaction pressure) [9,12]. This trend is also indicated by the specifications of a series of commercial flexible graphite heat-spreading sheets[1] SPREADERSHIELD, GrafTech International, Lakewood, OH). However, the opposite trend with the through-thickness thermal conductivity increasing with

[1] http://graftechled.com/GrafTech-LED-Files/TDS321—SPREADERSHIELD.pdf, as viewed on Jan. 24, 2014.

increasing density has also been reported [16]. The data points are fewer in Ref. [16] than Ref. [9]. This paper clarifies the effect of density (or compression pressure) on the through-thickness thermal conductivity.

The trend of the through-thickness thermal conductivity increasing with decreasing compaction pressure [9] suggests that the through-thickness electrical conductivity also increases with decreasing compaction pressure. This trend for the through-thickness electrical conductivity is indicated by the specifications of a series of commercial flexible graphite heat-spreading sheets[1] (SPREADERSHIELD, GrafTech International, Lakewood, OH). At solid contents beyond the percolation threshold, it was reported that the through-thickness electrical/thermal conductivity either does not change or increases with decreasing compaction pressure [4,12]. However, the unexpected opposite trend of the through-thickness electrical conductivity decreasing with decreasing compaction pressure has also been reported [14,15]. This opposite trend is probably because the resistance measurement was made by using the two-probe method (rather than the four-probe method) on a sandwich of the flexible graphite between metal surfaces [14,15]. Due to the two-probe method, the contact resistance is included in the measured resistance. As the pressure increases, the contact is probably tightened, so that the contact resistance is decreased. This paper clarifies the effect of the compaction pressure (i.e., the effect of the solid content) on the through-thickness electrical conductivity.

2. Experimental methods

2.1. Materials

Exfoliated graphite (worms) is obtained by rapid heating of expandable sulfuric-acid-intercalated graphite flake from Asbury (No. 3772) at 900 °C for 2 min with flowing nitrogen. The worms are of length 2–4 mm and specific surface area 41 m^2/g (measured by nitrogen adsorption using a Micromeritics ASAP 2010 instrument), corresponding to about 60 graphite layers (on the average) stacked in a cell wall in the cellular structure of the exfoliated graphite. This number of graphite layers is consistent with the previous report of approximately 68 graphite layers in a crystallite of exfoliated graphite with specific surface area 40 m^2/g [4]. With 60 graphite layers, the cell wall thickness would be about 20 nm. This cell wall thickness is consistent with the average graphite layer stack height (L_c = 24 nm) of graphite crystallites, as determined by X-ray diffraction for an exfoliated graphite compact [9]. The pressure used to compact the worms has almost no effect on L_c [9].

The increase in the pressure enhances the degree of preferred orientation of the graphite layers in the plane perpendicular to the direction of compaction, as shown by the increased intensity of the graphite 002 X-ray diffraction line [4,9]. The increase in the degree of preferred orientation is also indicated by the increase in the degree of electrical conductivity anisotropy [4], the increase in the degree of thermal conductivity anisotropy [12,13], and the increase in the degree of thermal/electrical conductivity anisotropy shown by the specifications of a series of commercial flexible graphite heat-spreading sheets[1] (SPREADERSHIELD, GrafTech International, Lakewood, OH).

2.2. Compaction method

The worms are compressed in a cylindrical steel mold of length 45 cm and inner diameter 31.8 mm by applying a uniaxial pressure via a matching steel piston. The entire thickness of a specimen is obtained in one compression stroke without interruption during the displacement of the piston. Each resulting specimen is a disc of diameter 31.8 mm and thickness ranging from 1.5 to 3.5 mm. Compression is conducted at pressures ranging from 0.71 to 11.7 MPa for 5 min to form exfoliated graphite compacts of density ranging from 0.047 to 0.669 g/cm^3 and carbon volume fraction (i.e., 1 – porosity) ranging from 2.08% to 29.6%. The density is determined by measurement of the mass and volume; at least four specimens are measured for each value of the fabrication pressure. For a given pressure (i.e., for a given density), specimens at three different thicknesses are prepared by using three different masses of worms, since the three thicknesses are needed for thermal conductivity measurement (Section 2.3). The fabrication pressures used are all low compared to most prior work on flexible graphite [9]. As a result, the density of the resulting compacts is quite low compared to that of flexible graphite (e.g., 1.1 g/cm^3 [9]).

2.3. Electrical conductivity measurement

The four-probe method is used for DC electrical resistance measurement. It involves two current contacts and two voltage contacts. Each of the two opposite surfaces of the specimen disc has a current contact that covers most of the circular surface and a small voltage contact that is at the center of the disc, such that the current and voltage contacts are not in electrical contact (Fig. 1). Each contact is made by silver paint in conjunction with aluminum foil (on top of the silver paint), which has an integral leg that protrudes to facilitate electrical connection. A high-precision multimeter (Keithley 2002) is used for the resistance measurement.

2.4. Thermal conductivity measurement

The thermal resistance between two copper cylinders (31.8 mm in diameter and 30.0 mm in height) with a specimen between them is measured using the Guarded Hot Plate Method, which is a steady-state method of heat flux measurement (ASTM Method D5470). The heat is provided by a 3.00×3.00 $in.^2$ (76.0×76.0 mm^2) square copper block that has two embedded heating coils (top block in Fig. 2). During the period of temperature rise, the heating rate is controlled at 3.2 °C/min by using a temperature controller. This copper block is in contact with one of the copper cylinders that sandwich the composite sample. The copper cylinders have a surface roughness of about 15 μm, which translates to a copper-specimen interface undulation of about 15 μm. The cooling is provided by a second 3.00×3.00 $in.^2$ copper block, which is cooled by running water that flows in and out of the block (bottom block in Fig. 2). This block is in contact with the other copper cylinder that is in contact with the specimen. An RTD

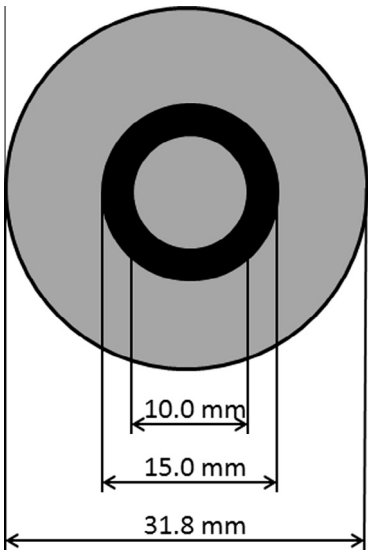

Fig. 1 – Electrical contact configuration for through-thickness electrical resistivity measurement. The four-probe method is used. Two electrical contacts are on each of the two opposite circular surfaces of the specimen disc. The contacts on the two surfaces do not touch. One of the two surfaces is shown. The two grey regions are electrical contacts. The outer contact (a ring that extends to the edge of the circular specimen surface) is for passing current. The inner contact (a solid circle) is for voltage measurement. The black region (a ring between the two grey regions) is the part of the specimen surface that is not covered by any electrical contact.

(resistance thermometer) probe (connected to Digi-Sense ThermoLogR RTD Thermometer from Fisher Scientific Co., with accuracy ±0.03 °C) is inserted in four drilled blind holes (T_1–T_4 in Fig. 2, each hole of diameter 3.3 mm) in the cylinder one after the other. Two of the four holes are in each of the copper cylinders. The temperature gradient is determined from $T_1 - T_2$ to $T_3 - T_4$. These two quantities should be equal at equilibrium, which is attained after holding the temperature of the heater at the desired value for 30 min. Equilibrium is assumed when the temperature variation is within ±0.1 °C in a period of 15 min. At equilibrium, the temperature of the hot square block is 100 °C, that of the cold square block is in the range 12–25 °C, while that of the top surface of the specimen is in the range 73–95 °C and the bottom surface 21–35 °C. Thus the average temperature of a sample is around 56 °C. The pressure in the direction perpendicular to the plane of the specimen is controlled by using a hydraulic press at a pressure of 0.46 MPa, except that a lower pressure of 0.15 MPa is used for the specimen with the lowest solid content (due to the softness of this specimen). The system is thermally insulated by wrapping laterally all the copper parts with layers of felt cloth.

In accordance with ASTM Method D5470, the heat flow Q is given by:

$$Q = \frac{\lambda A}{d_A}\Delta T, \tag{1}$$

where $\Delta T = T_1 - T_2 = T_3 - T_4$, λ is the thermal conductivity of copper, A is the area of the copper cylinder, and d_A is the distance between thermocouples T_1 and T_2 (i.e., 25.00 mm).

The temperature at the top surface of the specimen is T_A, which is assumed to be at the mid-point of the specimen-copper interface undulation. This temperature is given by:

$$T_A = T_2 - \frac{d_B}{d_A}(T_1 - T_2), \tag{2}$$

where d_B is the distance between thermocouple T_2 and the top surface of the specimen (i.e., 5.00 mm).

The temperature at the bottom surface of the specimen is T_D, which is again assumed to be at the mid-point of the specimen-copper interface undulation amplitude. This temperature is given by:

$$T_D = T_3 + \frac{d_D}{d_C}(T_3 - T_4), \tag{3}$$

where d_D is the distance between thermocouple T_3 and the bottom surface of the specimen (i.e., 5.0 mm) and d_C is the distance between thermocouples T_3 and T_4 (i.e., 25.00 mm).The two-dimensional thermal resistivity θ is given by:

$$\theta = (T_A - T_D)\frac{A}{Q}, \tag{4}$$

Note that insertion of Eq. (1) into Eq. (4) causes cancellation of the term A, so that θ is independent of A.

Each type of specimen is tested at three different thicknesses. For each thickness, four specimens are tested. Testing at multiple thicknesses allows the thermal resistance of the specimen-copper interface to be decoupled from that of the specimen. The thermal conductivity is given by the reciprocal of the slope of the plot of the thermal resistivity versus the thickness (Fig. 3). The linearity of this plot shows that the use of three thicknesses is adequate for determining the slope of the plot. The linearity of such plots has been previously reported for carbon fiber epoxy-matrix composites by using the same testing method and set-up [17].

3. Results

The solid contents studied (Table 1) are all beyond the percolation threshold, in contrast to prior work around the percolation threshold [4]. The lowest solid content studied in this work is just above the threshold. Table 1 shows the results on the through-thickness thermal and electrical conductivities.

The through-thickness electrical conductivity decreases with increasing density. This trend is consistent with the trend reported for exfoliated graphite compacts around the percolation threshold [4] and is also consistent with that exhibited by the series of GrafTech SPREADERSHIELD flexible graphite products. However, it is opposite to that in Refs. [14,15], thus confirming the notion made in the Introduction concerning the inaccuracy of the results in these two papers due to the use of the two-probe method to measure the resistance.

The Rule of Mixtures, with the graphite and air considered to be thermal/electrical resistors in parallel along the through-thickness direction, is used to model the through-thickness

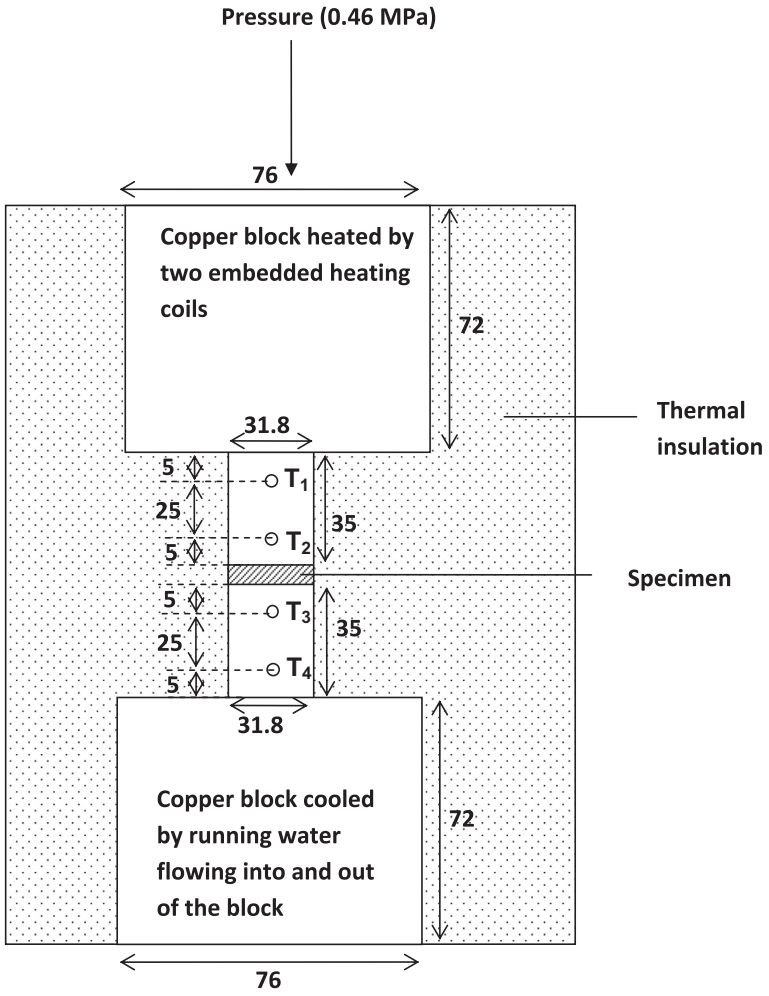

Fig. 2 – Through-thickness thermal conductivity measurement set-up. The copper blocks for heating (at the top) and cooling (at the bottom) are square in cross section. Between them are two copper cylinders, each having two holes for thermocouple insertion. Between the two cylinders is the specimen under evaluation. All dimensions are in mm.

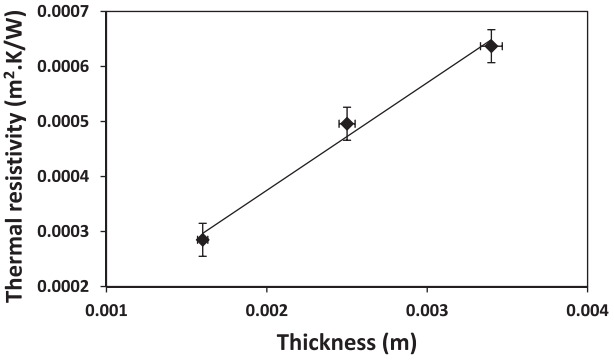

Fig. 3 – Thermal resistivity vs. thickness for exfoliated graphite compact with 19.5 vol.% solid. The linearity is similarly observed for compacts with other solid contents. Such linearity is obtained for all solid contents. The slope of the plot equals the reciprocal of the thermal conductivity.

electrical/thermal conductivity of exfoliated graphite compacts, i.e.,

$$\sigma = \upsilon_s \sigma_s, \quad (5)$$

where σ is the thermal/electrical conductivity of the overall compact, σ_s is the thermal/electrical conductivity of the solid part of the compact, and υ_s is the volume fraction of solid (graphite) in the compact. In deriving Eq. (5), the conductivity of air was assumed to be zero. The series configuration of the conductors does not work, because of the zero conductivity of the air. Based on Eq. (5), the electrical conductivity of the graphite (solid) part of the compact is calculated and shown in Table 1. This conductivity decreases (from 153 to 7.16 kS/m) with increasing density even more significantly than the measured conductivity of the overall compact (from 3.21 to 2.12 kS/m). This means that the structure of the solid part changes significantly as the density increases. This structural change involves an increase in the degree of preferred orientation of the graphite layers in the plane perpendicular to the compaction direction as the density increases. The increase in the degree of preferred orientation has been previously reported, as based on X-ray diffraction results [9].

Ref. [4] reports that the measured electrical conductivity of the overall compact (isotropic due to the unusually low degree of compaction) is about 0.3–1.0 kS/m in both in-plane and through-thickness directions for a solid content of 1–2 vol.%

Table 1 – Through-thickness electrical and thermal conduction parameters of exfoliated graphite compacts fabricated at different compaction pressures. The last column is for a commercial flexible graphite material.

Solid volume fraction (%)		2.08 ± 0.12	7.02 ± 0.16	12.8 ± 0.2	19.5 ± 0.3	25.5 ± 0.3	29.6 ± 0.4	84
Compaction pressure (MPa)		0.71	2.49	5.01	7.84	9.63	11.7	/
Density (g/cm^3)		0.047 ± 0.003	0.159 ± 0.004	0.289 ± 0.004	0.441 ± 0.006	0.576 ± 0.007	0.669 ± 0.009	1.9[c]
Electrical conductivity (kS/m)	Overall	3.21 ± 0.15	2.87 ± 0.14	2.59 ± 0.06	2.38 ± 0.06	2.20 ± 0.03	2.12 ± 0.03	0.5[c]
	Solid part[a]	153 ± 7	41.0 ± 2.2	20.2 ± 0.5	12.2 ± 0.5	8.64 ± 0.10	7.16 ± 0.09	0.59
	Solid part[b]	229 ± 14	59.9 ± 3.0	29.1 ± 0.7	17.1 ± 0.6	11.8 ± 0.2	10.1 ± 0.2	0.64
Thermal conductivity (W/(m K))	Overall	7.65 ± 0.39	7.01 ± 0.44	6.21 ± 0.24	5.50 ± 0.22	4.88 ± 0.10	4.61 ± 0.09	3.4[c]
	Solid part[a]	368 ± 19	99.9 ± 6.3	48.5 ± 1.9	28.2 ± 1.1	19.1 ± 0.4	15.6 ± 0.3	4.0
	Solid part[b]	548 ± 28	146 ± 9	75.8 ± 2.9	39.6 ± 1.6	26.3 ± 0.5	21.1 ± 0.4	4.3
Fraction (f) of through-thickness conduction path that is a-axis	Electrical[a]	0.991 ± 0.001	0.962 ± 0.001	0.919 ± 0.001	0.858 ± 0.001	0.790 ± 0.002	0.742 ± 0.003	0.000
	Electrical[b]	0.994 ± 0.001	0.972 ± 0.001	0.945 ± 0.001	0.893 ± 0.002	0.838 ± 0.003	0.798 ± 0.003	0.000
	Thermal[a]	0.996 ± 0.001	0.985 ± 0.001	0.971 ± 0.001	0.951 ± 0.001	0.931 ± 0.001	0.917 ± 0.001	0.000
	Thermal[b]	0.997 ± 0.001	0.989 ± 0.001	0.978 ± 0.001	0.962 ± 0.001	0.946 ± 0.001	0.937 ± 0.002	0.000
Ratio of thermal conductivity to electrical conductivity (10^{-3} W Ω/K)		2.38 ± 0.17	2.44 ± 0.19	2.40 ± 0.11	2.32 ± 0.11	2.21 ± 0.05	2.17 ± 0.05	0.68
Lorentz number at 298 K (10^{-6} W Ω/K^2)		7.98 ± 0.56	8.19 ± 0.59	8.05 ± 0.37	7.79 ± 0.37	7.43 ± 0.16	7.31 ± 0.14	2.3

[a] Back calculated from the measured value for the overall specimen by using the Rule of Mixtures for conductors (carbon and air) in parallel (Eq. (5)).
[b] Back calculated from the measured value for the overall specimen by using the Hashin–Shtrikman model (upper bound) (Eq. (6)) [12,18].
[c] SPREADERSHIELD SS1500, http://graftechled.com/GrafTech-LED-Files/TDS321—SPREADERSHIELD.pdf, as viewed on Jan. 24, 2014.

(density 0.02–0.04 g/cm^3, corresponding to the regime around the conduction percolation threshold). These ranges of the solid content and the density are below those of this work (2–30 vol.%, 0.05–0.67 g/cm^3). As expected, the measured conductivity reported in Ref. [4] is lower than that of this work (2.1–3.2 kS/m).

The Effective Medium Theory considers two kinds of grains (i.e., two phases, which are, in this case, graphite and air) that differ in the electrical conductivity in a material that is in the form of a two-phase mixture and assumes that the medium surrounding each kind of grain is uniform, exhibiting property values that are equal to those of the mixture [4]. Furthermore, the theory assumes that the grains of each phase are homogeneously distributed [4]. By using the Effective Medium Theory to model the electrical conductivity of the abovementioned isotropic exfoliated graphite compacts, Ref. [4] deduced from the measured conductivity of the compact the value of 1000 kS/m for the electrical conductivity of the graphite (solid) part of the compact. This value is higher than the value of 153 kS/m obtained in this work based on the Rule of Mixtures for the exfoliated graphite compact with a solid content of 2 vol.%. The difference is consistent with the low solid content in Ref. [4] compared to this work and the fact that the electrical conductivity of the solid (graphite) part of the compact decreases with increasing density (Table 1).

The results of modeling based on the Effective Medium Theory [4] and that based on the Rule of Mixtures (this work) are roughly consistent, in spite of the solid content ranges used in the two models are different. The Effective Medium Theory is limited to the range of solid content around the percolation threshold, because the degree of conductivity anisotropy increases with the solid content when the solid content is above the threshold [4]. The Rule of Mixtures is attractive in that it is applicable to the full range of solid content, including the range above the percolation threshold. The range above the threshold is practically more important than that around or below the threshold, due to the high conductivity above the threshold.

The Rule of Mixtures is too simplistic because it assumes that the conduction paths are all parallel in the direction of compaction. A more advanced model is the Hashin–Shtrikman model (upper bound) [12,18], i.e.,

$$\sigma = \sigma_s\left[1 - 3\left(\frac{\beta}{2+\beta}\right)\right], \tag{6}$$

where σ is the overall thermal/electrical conductivity, σ_s is the thermal/electrical conductivity of the solid part, and β is the porosity, i.e., 1 – solid volume fraction. Table 1 shows that the Rule of Mixtures gives lower values of the thermal/electrical conductivities of the solid part than the Hashin–Shtrikman model. The relatively low values of the conductivity of the solid part based on the Rule of Mixtures are due to the idealistic assumption in this model that the conduction paths are all parallel in the direction of compaction. The values based on the Hashin–Shtrikman model are more realistic. However, the two models give results that are comparable.

The thermal conductivity decreases with increasing density (Table 1). This trend agrees with that reported in Ref. [9], but is opposite to that in Ref. [14], thereby confirming

the notion mentioned in the Introduction concerning the relatively low reliability of the trend in Ref. [12]. The thermal conductivity of the solid (graphite) part, as calculated based on either the Hashin–Shtrikman model (Eq. (6)) or the Rule of Mixtures (resistors in parallel) (Eq. (5)), reflects the structure of the solid part. This thermal conductivity decreases [from 550 to 21 W/(m K) based on the Hashin–Shtrikman model and from 370 to 16 W/(m K) based on the Rule of Mixtures] with increasing density even more significantly than the measured thermal conductivity of the overall compact (from 8 to 5 W/(m K)). This decrease is due to a structural change of the solid part. This change is attributed to an increase in the degree of preferred orientation of the graphite layers in the plane perpendicular to the compaction direction, as also indicated by the decrease of the electrical conductivity of the solid part with increasing density (Table 1). Because the solid part amounts to a small volume fraction of the compact, the structural change of the solid part does not affect the thermal/electrical conductivity of the overall compact as much as that of the solid part.

The higher is the compaction pressure, the greater is the solid content, and the higher is the degree of preferred orientation. The scientific origin of the observed decrease in the thermal/electrical conductivity of the solid part with increasing solid content relates to the degree of preferred orientation rather than the solid content.

Fig. 4 shows that the thermal and electrical conductivities of the solid part of the compact decrease monotonically with increasing solid content, such that they abruptly decrease with increasing solid content at solid contents in the range 2–7 vol.%, whereas those of the overall compact decrease monotonically and smoothly with increasing solid content for the full range of solid content from 2 to 30 vol.%. This means that the thermal/electrical conductivity of the solid part is very sensitive to the degree of preferred orientation in the regime of low degree of preferred orientation. This is probably because the regime of low degree of preferred orientation is close to the conduction percolation threshold, which is at 1–2 vol.% [4]. Above the percolation threshold, the through-thickness conductivities decrease with increasing solid content, due to the increasing degree of anisotropy. The smoothness of the curves for the thermal and electrical conductivities of the overall compact (Fig. 4(a)) is probably because the conduction percolation effect is diluted by the large volume fraction of air voids in the compact. The strong correlation between the overall thermal and electrical conductivities (Fig. 4(a)) and that between the thermal and electrical conductivities of the solid part (Fig. 4(b) and (c)) are also shown by the similarity of the shape of the curves.

The thermal conductivity of the solid part of the exfoliated graphite compact is as high as 550 and 370 W/(m K) for the Hashin–Shtrikman model and the Rule of Mixtures (parallel) model respectively. These highest values are exhibited by the compact with the lowest solid content of 2.1 vol.% (Table 1). These values are higher than the value of 95 W/(m K) for the thermal conductivity of AXF-5Q polycrystalline graphite[2] and

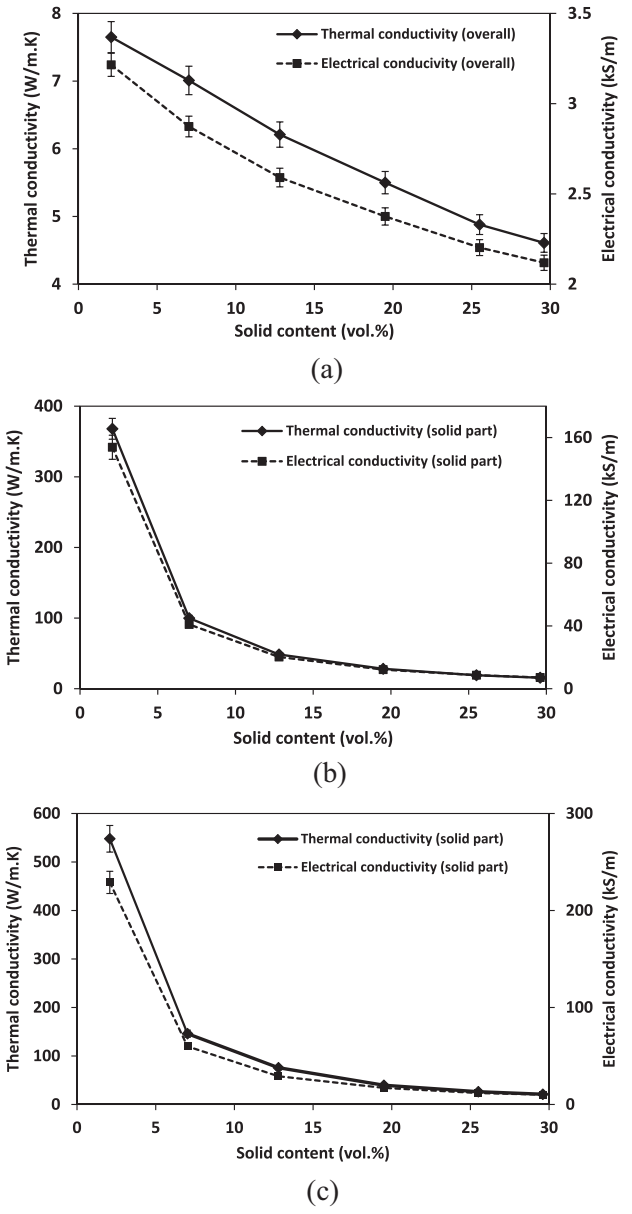

Fig. 4 – Effect of the solid content on the thermal and electrical conductivities of exfoliated graphite. (a) The thermal and electrical conductivities of the overall compact. (b) The thermal and electrical conductivities of the solid part of the compact, as obtained based on the Rule of Mixtures. (c) The thermal and electrical conductivities of the solid part of the compact, as obtained based on the Hashin–Shtrikman model.

are much higher than the value of 8 ± 1 W/(m K) for the through-thickness direction of HOPG,[3] but are lower than the value of 1700 ± 100 W/(m K) for the in-plane direction of HOPG.[3] The degree of preferred orientation of the graphite layers in the plane of HOPG is very high, thus resulting in a very high value of the in-plane thermal conductivity. The

[2] http://www.poco.com/MaterialsandServices/Graphite/IndustrialGrades/AXF5Q.aspx, as viewed on Jan. 22, 2014.
[3] http://www.optigraph.eu/basics.html, as reviewed on Jan. 22, 2014.

through-thickness thermal conductivity of the graphite (solid) part of the exfoliated graphite compact is lower than the in-plane thermal conductivity of HOPG by a factor of 5 only. These results suggest that the *a*-axis conduction path significantly contributes to the through-thickness thermal conduction of exfoliated graphite compacts. This notion is consistent with the fact that the worms are interconnected in an exfoliated graphite compact.

The electrical conductivity of the solid part of the exfoliated graphite compact is as high as 230 and 150 kS/m for the Hashin–Shtrikman model and the Rule of Mixtures (parallel) model respectively. These highest values are exhibited by the compact with the lowest solid content of 2.1 vol.% (Table 1). These values are lower than the value of 2083 kS/m for the in-plane electrical conductivity of highly oriented pyrolytic graphite (HOPG[2]), but are higher than the value of 68 kS/m for polycrystalline graphite (AXF-5Q, Poco Graphite, Inc.[2]). The degree of preferred orientation of the graphite layers in the plane of HOPG is very high, thus resulting in a very high value of the in-plane electrical conductivity. The through-thickness electrical conductivity of the graphite (solid) part of the exfoliated graphite compact is lower than the in-plane conductivity of HOPG by only an order of magnitude. These results suggest that the *a*-axis conduction path significantly contributes to the through-thickness electrical conduction of exfoliated graphite compacts.

The significant contribution of the *a*-axis conduction path to the through-thickness thermal/electrical conduction of exfoliated graphite compacts means that the thermal/electrical connectivity is substantial in the through-thickness direction and that the through-thickness connectivity substantially involves linkages of segments along the *a*-axis. These segments are graphite crystallites that are at various angles relative to the direction of compaction [4], although there is a degree of preferred orientation of the graphite layers in the plane perpendicular to the compaction direction. The lower is the degree of preferred orientation, the less tortuous is the *a*-axis conduction path in the compaction direction and hence the higher is the conductivity in the compaction direction. The higher is the degree of preferred orientation, the less tortuous is the *a*-axis conduction path in the plane perpendicular to the compaction direction and hence the higher is the in-plane conductivity. As a consequence, the degree of anisotropy increases with the degree of preferred orientation. In the plane perpendicular to the compaction direction, connectivity of the *a*-axis conduction path obviously occurs above the percolation threshold [4], as indicated by the high in-plane thermal and electrical conductivities [9]. This work shows that such connectivity also occurs in the through-thickness direction above the percolation threshold, in spite of the anisotropy. However, due to the anisotropy, the degree of connectivity is lower (i.e., the tortuosity of the *a*-axis conduction path is greater) in the through-thickness direction than the in-plane direction. This finding is to be distinguished from connectivity in both in-plane and through-thickness directions previously reported for exfoliated graphite compacts that are isotropic [4].

The through-thickness thermal/electrical conductivity of the solid part decreases with increasing solid content, due to the increasing degree of preferred orientation. Thus, a simple model in which the conductivity is inversely related to the solid content is considered. This model means that the product of the conductivity and the solid content is a constant. If the Rule of Mixtures is used to deduce the conductivity of the solid part, this product is in fact equal to the overall conductivity, since the conductivity of the solid part is obtained by dividing the overall conductivity by the solid content (Eq. (5)). Table 1 shows that this product is roughly a constant, being 4.6–7.7 W/(m K) in relation to the thermal conductivity and 2.1–3.2 kS/m in relation to the electrical conductivity. This analysis supports the notion that the degree of preferred orientation governs the through-thickness thermal/electrical conductivity of the solid part of the compact.

The fraction *f* of through-thickness conduction path that is along the *a*-axis is obtained by using the Rule of Mixtures for thermal/electrical conductors in series (a configuration that is consistent with the notion that *a*-axis conduction path segments and *c*-axis conduction path segments are connected to form a tortuous path that has the overall direction along the through-thickness direction, which is the direction under consideration), i.e.,

$$\frac{1}{\sigma_s} = \frac{f}{\sigma_{sa}} + \frac{(1-f)}{\sigma_{sc}}, \tag{7}$$

where σ_s is the thermal/electrical conductivity of the solid part, σ_{sa} is the *a*-axis thermal/electrical conductivity of the solid part of the reference (described below) and σ_{sc} is the *c*-axis thermal/electrical conductivity of the solid part of the reference. The *f* value describes the degree of preferred orientation of the graphite layers along the through-thickness direction. This value is obviously high when the degree of preferred orientation of the graphite layers in the plane perpendicular to the through-thickness direction is low. In contrast, prior work [12] considers the fraction *f* in terms of the Rule of Mixtures for conductors in parallel. The parallel model [$\sigma_s = f\ \sigma_{sa} + (1-f)\ \sigma_{sc}$] is found in this work to give unreasonably small values of *f*, i.e., up to 0.067 in relation to electrical conduction and up to 0.20 in relation to thermal conduction. For a geometrical point of view, the parallel model is not as suitable as the series model, because the parallel model considers *a*-axis and *c*-axis segments to be parallel to one another, such that these segments are not connected.

The reference is SPREADERSHIELD SS1500, which is flexible graphite that is high in density (1.9 g/cm^3,[4] corresponding to a solid content of 84%) and as anisotropic as HOPG.[3] Due to its strong thermal conductivity anisotropy (440,[1] compared to 210 for HOPG[3]) and strong electrical conductivity anisotropy (3800,[1] compared to 4000 for HOPG[3]), it is assumed to conduct along the through-thickness direction only by the *c*-axis path, i.e., without involving the *a*-axis path. Hence, the *c*-axis conductivity of the reference is given by its through-thickness conductivity, whereas the *a*-axis conductivity of the reference is given by its in-plane conductivity. The conductivity of the solid part of the reference is obtained using the Rule of

[4] http://technicome.info/composants/c_specif/gra/Catalogue%20ETM.pdf, as viewed on Jan. 29, 2014.

Mixtures by dividing the overall conductivity of the reference by the solid volume fraction of the reference (Eq. (5)). The overall in-plane and through-thickness thermal conductivities of the reference are 1500 and 3.4 W/(m K) respectively.[1] The overall in-plane and through-thickness electrical conductivities of the reference are 1900 and 0.5 kS/m respectively.[1]

Table 1 shows that f decreases with increasing solid content, such that it decreases from 0.997 to 0.937 (Hashin–Shtrikman model) or from 0.996 to 0.917 (Rule of Mixtures) in relation to thermal conduction and from 0.994 to 0.798 (Hashin–Shtrikman model) or from 0.991 to 0.742 (Rule of Mixtures) in relation to electrical conduction. The corresponding f values are slightly higher for the Hashin–Shtrikman model than the Rule of Mixtures. All the values are above 0.7. These high values mean that the a-axis conduction path predominates both thermal and electrical conduction in the through-thickness direction. This means that the c-axis path contributes in a very minor way. The predominance of the a-axis path is consistent with the numerous observations described above, as well as the Lorentz number consideration described below.

At any solid content, f is higher for thermal conduction than electrical conduction, such that the difference becomes more significant as the solid content increases. This means that the a-axis path is more important for thermal conduction than electrical conduction. These differences between thermal and electrical conduction are because of the phonon mechanism of thermal conduction [19–22], in contrast to the electronic mechanism of electrical conduction. The difference in Debye temperature between the a-axis and c-axis of graphite is large [21].

Fig. 5 shows that the f value decreases with increasing solid content, whether the electrical conductivity or the thermal conductivity is considered. This trend is due to the fact that the degree of preferred orientation of the graphite layers increases with increasing solid content (i.e., with increasing compaction pressure). The decrease in the f value with increasing solid content is more significant for the electrical conductivity than the thermal conductivity. This is because the anisotropy is greater for the electrical conductivity than for the thermal conductivity. For SPREADERSHIELD SS1500, which corresponds to the case of a high degree of anisotropy, the thermal conductivity anisotropy is 440, whereas the electrical conductivity anisotropy is 3800.[1]

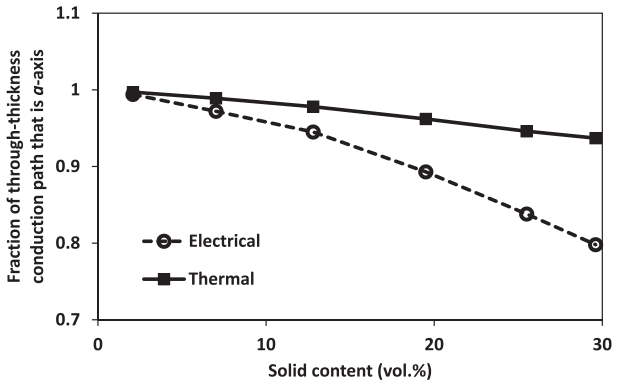

Fig. 5 – Correlation of the fraction f of through-thickness thermal/electrical conduction path that is a-axis (obtained by using the Hashin–Shtrikman model) with the solid content.

Flexible graphite currently marketed for in-plane heat spreading (SPREADERSHIELD, GrafTech International, Lakewood, OH) exhibits through-thickness thermal conductivity up to 4.5 W/(m K) and through-thickness electrical conductivity up to 2.86 kS/m (given by Grade SS300).[1] This value for the thermal conductivity is comparable to the value [4.6 W/(m K), Table 1] obtained in this work for the overall exfoliated graphite compact with the highest solid content of 29.6 vol.%. By decreasing the solid content, this work has achieved through-thickness thermal conductivity up to 8 W/(m K) (Table 1) for the overall compact. The value of 2.86 kS/m for the through-thickness electrical conductivity of SPREADERSHIELD SS300[1] is essentially equal to the value obtained in this work for the overall exfoliated graphite compact with the solid content of 7.0 vol.%. By decreasing the solid content, this work has achieved through-thickness electrical conductivity up to 3.21 kS/m (Table 1) for the overall compact.

The exfoliated graphite compact at the lowest solid content of 2.1 vol.% is most attractive in terms of the high electrical conductivity (3.21 kS/m for the overall compact) and the high thermal conductivity [8 W/(m K) for the overall compact]. Almost as attractive is the compact with the second lowest solid content of 7.0 vol.%. These values are attractive for applications as biopolar plates of fuel cells and flow batteries. The compact at the lowest solid content of 2.1 vol.% is mechanically soft, so the compact at the second lowest solid content of 7.0 vol.% is more suitable for applications.

Polycrystalline graphite (AXF-5Q, Poco Graphite, Inc.)[2] exhibits even higher electrical and thermal conductivities [68 kS/m and (95 W/(m K) respectively] than the overall exfoliated graphite compacts, but its shaping is more difficult. Metals tend to exhibit yet higher electrical and thermal conductivities (e.g., 58,000 kS/m and 388 W/(m K) respectively for copper [23]), but they suffer from (i) the inadequate ability to withstand harsh chemical environments, such as the high-temperature acidic environment that is typically encountered in fuel cells, (ii) the high values of the coefficient of thermal expansion compared to those of carbon materials, and (iii) the difficulty of shaping compared to exfoliated graphite compacts. Nevertheless, the solid part of the exfoliated graphite exhibits thermal conductivity [up to 550 W/(m K) using the Hashin–Shtrikman model and up to 370 W/(m K) using the Rule of Mixtures] that is comparable to that of copper.

4. Discussion

The strong and essentially linear correlation between the thermal and electrical conductivities is shown in Fig. 6. The approximate linearity means that both thermal conduction and electrical conduction are similarly governed by the degree of preferred orientation. In other words, the conduction mechanism is not affected by the preferred orientation degree. In graphite, it is well-known that the a-axis thermal/electrical conductivity is much higher than the c-axis thermal/electrical conductivity. The linearity does not imply that the conduction mechanism is the same for thermal

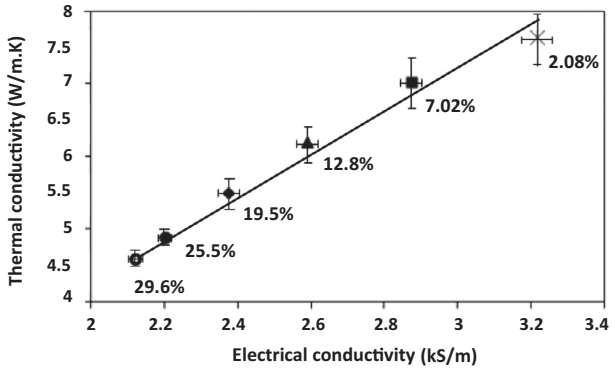

Fig. 6 – Correlation of the thermal and electrical conductivities, both in the through-thickness direction. The volume fraction solid is shown next to each data point.

and electrical conduction. In fact, the electrical conduction is governed by electrons/holes, whereas the thermal conduction is governed by phonons [19–22]. Due to the data scatter, the linearity is approximate and the curve could be non-linear to a limited degree. The limited non-linearity may be due to the fact that, in graphite, the electrical conductivity anisotropy (4000 for HOPG[3]) is higher than the thermal conductivity anisotropy (210 for HOPG[3]).

Table 1 shows the through-thickness Lorentz number L, which is defined as:

$$L = \frac{\kappa}{\sigma T}, \tag{8}$$

where T is the temperature in K (298 K for room temperature), κ is the thermal conductivity, and σ is the electrical conductivity. The L value for exfoliated graphite compacts in the through-thickness direction has not been previously reported. The a-axis conduction path contributes significantly to the conduction in the in-plane direction of the compact, as shown by the high values of the in-plane thermal conductivity (100–600 W/(m K) [9]) and the high values of the in-plane electrical conductivity (50–250 kS/m [9]). Based on the room-temperature values of the in-plane thermal and electrical conductivities of flexible graphite of various densities ranging from 0.55 to 1.8 g/cm^3 [9], the in-plane L value is calculated in the present work to be in the range from 5.6×10^{-6} to 6.2×10^{-6} W Ω/K^2; at the lowest density of 0.55 g/cm^3 (close to the highest density of 0.67 g/cm^3 in the present work), in-plane L equals 5.6×10^{-6} W Ω/K^2. For the exfoliated graphite compacts of this work, the error in through-thickness L decreases with increasing density (Table 1), so the through-thickness L value of 7.3×10^{-6} W Ω/K^2 obtained at the highest density is taken to be the most accurate value. Hence, the L values for the in-plane and through-thickness directions are quite close. (The difference is at least partly due to the difference in the acid intercalate species and possibly also due to a difference in the degree of exfoliation.) The similarity supports the notion that the a-axis conduction path predominates the conduction in the through-thickness direction of the compact.

With the data scatter taken into consideration, the through-thickness L essentially does not vary with the density (Table 1). The in-plane L also essentially does not vary with the density [9]. As the degree of preferred orientation depends on the density, this means that the degree of preferred orientation has little effect, if any, on the through-thickness or in-plane L value. This means that phonons govern thermal conduction to similar degrees for all the degrees of preferred orientation studied. The a-axis conduction path predominates the through-thickness thermal/electrical conduction for all of the degrees of preferred orientation associated with the various densities of the exfoliated graphite compacts.

Ref. [22] reports the correlation between the in-plane thermal and electrical conductivities of flexible graphite, but it does not consider the degree of linearity in the correlation. The L values obtained are high compared to that of metals (2.45×10^{-8} W Ω/K^2). This led Ref. [22] to conclude that most of the in-plane thermal conduction in flexible graphite is due to phonons.

In contrast to exfoliated graphite compacts, polycrystalline graphite exhibits relatively little preferred orientation. The Lorentz number of exfoliated graphite compacts is close to that of polycrystalline graphite (AXF-5Q, Poco Graphite, Inc., 4.7×10^{-6} W Ω/K^2).[2] For Acheson polycrystalline graphite, the L value (1.1×10^{-6} W Ω/K^2 [24]) is similar. These similarities are consistent with the notion that phonons govern thermal conduction to similar degrees for various degrees of preferred orientation. In addition, it supports the notion that the a-axis conduction path predominates the conduction in the exfoliate graphite compacts. In case of AXF-5Q polycrystalline graphite, the thermal and electrical conductivities are both high (95 W/(m K) and 68 kS/m respectively),[2] further indicating the significant contribution of the a-axis conduction path.

The HOPG exhibits through-thickness thermal conductivity (8 ± 1 W/(m K)[3]) that is comparable to that of the overall exfoliated graphite compacts of low density, but its through-thickness electrical conductivity (0.5 kS/m[3]) is much lower than that of the exfoliated graphite compacts. The HOPG is highly anisotropic, with high in-plane thermal conductivity (1700 ± 100 W/(m K)[3]) and high in-plane electrical conductivity (2083 ± 104 kS/m[3]). The low through-thickness electrical conductivity (0.5 kS/m[3]) of HOPG is attributed to the high degree of in-plane preferred orientation in HOPG.

The Lorentz number of exfoliated graphite (7.3×10^{-6} W Ω/K^2) is close to that for in-plane HOPG (2.9×10^{-6} W Ω/K^2[23]) and below that for through-thickness HOPG (5.4×10^{-5} W Ω/K^2[23]). This further supports the notion that the a-axis conduction path significantly contributes to the through-thickness thermal conduction of exfoliated graphite compacts. The through-thickness direction of HOPG substantially involves c-axis conduction and the through-thickness electrical conductivity of HOPG is very low [5×10^2 (Ω m)$^{-1}$, compared to 2×10^6 (Ω m)$^{-1}$ for the in-plane direction of HOPG.[3]

The in-plane L values of flexible graphite at 4.2 K have been reported as 71×10^{-8} and 10.5×10^{-8} W Ω/K^2 for the transverse direction (the in-plane direction perpendicular to the in-plane rolling direction) and the rolling direction (with the compaction of the worms conducted during rolling) respectively [25]. Due to the large difference in temperature between Ref. [25] (4.2 K) and this work (room temperature),

comparison of the L values of Ref. [25] and this work is not suitable.

Figs. 7 and 8 show that the fraction f of through-thickness electrical/thermal conduction path that is a-axis increases smoothly with increasing overall electrical/thermal conductivity of the overall compact, but increases abruptly with increasing electrical/thermal conductivity of the solid part of the compact (as obtained by using the Hashin–Shtrikman model). For both the overall conductivity (which depends on both the solid volume fraction and the conductivity of the solid part of the compact) and the conductivity of the solid part, the conductivity becomes more sensitive to the f value as the f value increases. In other words, the through-thickness conductivity becomes more sensitive to the preferred orientation of the graphite layers as the preferred orientation of the graphite layers in the plane perpendicular to the compaction direction decreases. Furthermore, the conductivity of the solid part is strongly affected by the f value only when the f value is very high, whereas the conductivity of the overall compact is moderately affected by the f value for the whole range of f values. This means that the conductivity of the solid part is highly sensitive to the preferred orientation only when the preferred orientation of the graphite layers in the plane perpendicular to the compaction direction is in the very low range, whereas the conductivity of the overall compact is moderately sensitive to the preferred orientation for the whole range of preferred orientation degree. In order to achieve a high value [>60 kS/m and 140 W/(m K), according to the Hashin–Shtrikman model] of the electrical/thermal conductivity of the solid part, the f value must exceed 0.95.

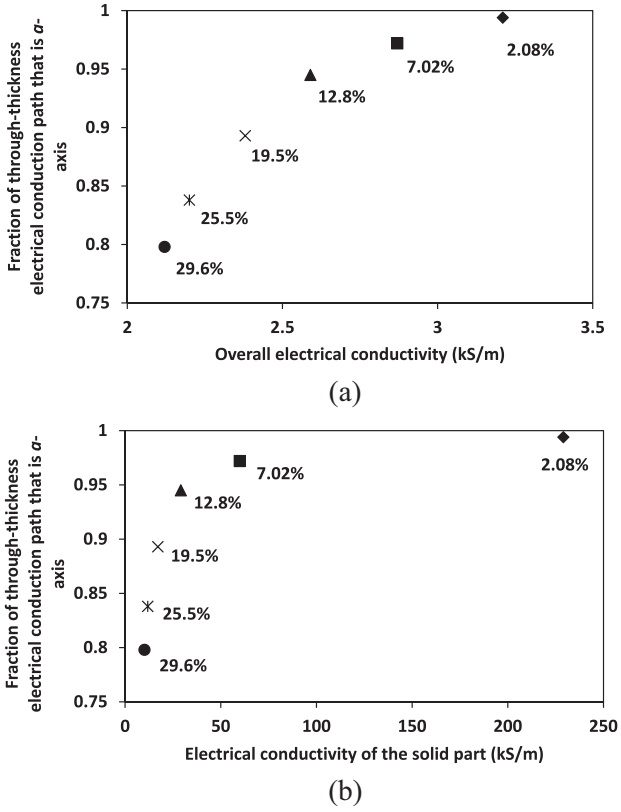

Fig. 7 – Correlation of the fraction of through-thickness electrical conduction path that is a-axis with the electrical conductivity. The volume fraction solid is shown next to each data point. (a) The overall conductivity of the compact. (b) The conductivity of the sold part of the compact, obtained by using the Hashin–Shtrikman model.

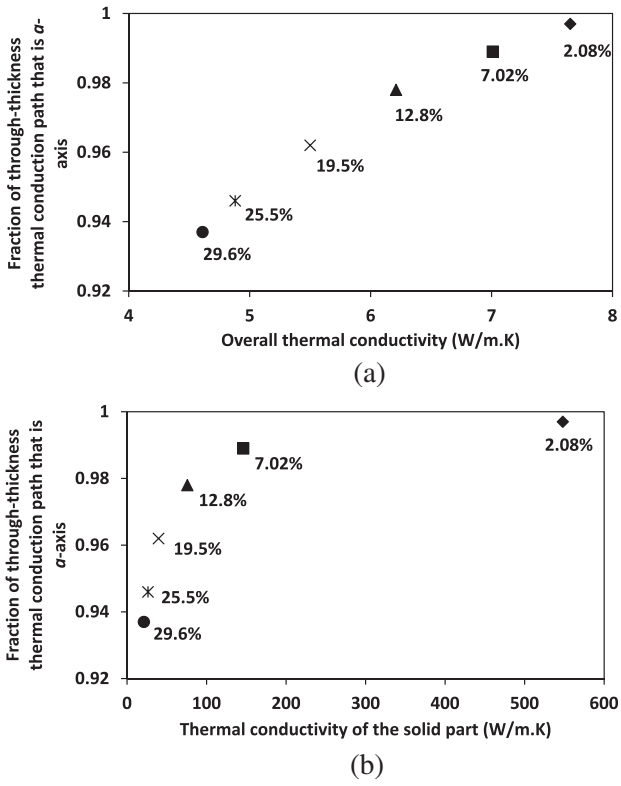

Fig. 8 – Correlation of the fraction of through-thickness thermal conduction path that is a-axis with the thermal conductivity. The volume fraction solid is shown next to each data point. (a) The overall conductivity of the compact. (b) The conductivity of the solid part of the compact, obtained by using the Hashin–Shtrikman model.

The highest electrical and thermal conductivities obtained are toward, but still below, the industrial targets. The electrical conductivity is particularly in need of improvement. In addition to further enhancement of the conductivities, future work can involve measurement of the in-plane conductivities, mechanical properties, hydrogen gas permeability and other properties that are relevant to bipolar plate applications.

5. Conclusion

It is well-known that an increase in compaction pressure increases both the density and the degree of preferred orientation of the graphite layers perpendicular to the compaction direction. This work provides the decoupling of these two contributions to the effect of the compaction pressure in the range corresponding to the graphite volume fraction above the percolation threshold and shows the effectiveness of the decoupling by using either the Hashin–Shtrikman model or the Rule of Mixtures (for thermal/electrical resistors in parallel). The results based on the two models for the

conductivities of the solid part of the compact are comparable, but are higher for those based on the Hashin–Shtrikman model. The large changes in the thermal and electrical conductivities of the solid part of the compact as the density increases supports the significant change in the degree of preferred orientation in the solid part as the density increases.

The thermal and electrical conductivities become more sensitive to the preferred orientation of the graphite layers as the preferred orientation of the graphite layers in the plane perpendicular to the compaction direction decreases. In order to achieve a high value [>60 kS/m and 140 W/(m K), according to the Hashin–Shtrikman model] of the electrical/thermal conductivity of the solid part, the fraction f of through-thickness conduction path that is along the a-axis must exceed 0.95.

In the through-thickness direction, high thermal conductivity [up to 550 and 370 W/(m K) for the Hashin–Shtrikman model and the Rule of Mixtures respectively] and high electrical conductivity (up to 230 and 150 kS/m for the Hashin–Shtrikman model and the Rule of Mixtures respectively, above those of polycrystalline graphite AXF-5Q) are exhibited by the solid (graphite) part of the compact. The compaction-related variation in the conductivities of the solid part is large, due to the compaction-related variation in the degree of preferred orientation of the graphite layers.

The electrical and thermal conductivities of exfoliated graphite compacts in the through-thickness direction (i.e., the compaction direction) decrease with increasing degree of compaction (i.e., with increasing density in the range beyond the percolation threshold), such that they are essentially linearly correlated in accordance with the Wiedemann–Franz Law. The linearity is because both thermal conduction and electrical conduction are similarly governed by the degree of preferred orientation, which is in turn governed by the degree of compaction.

The a-axis conduction path predominates both the through-thickness and in-plane thermal/electrical conduction, due to the thermal/electrical connectivity in the structure of an exfoliated graphite compact. The a-axis contribution to the conduction is higher for thermal conduction than electrical conduction. The fraction of through-thickness conduction path that is a-axis decreases with increasing compaction, from 0.997 to 0.937 and from 0.994 to 0.798 for thermal and electrical conduction respectively. These ranges are obtained by using the Hashin–Shtrikman model and are almost the same when the Rule of Mixtures is used instead. This means that the c-axis path contributes in a very minor way to the through-thickness conduction.

The Lorentz number of exfoliated graphite (7.3×10^{-6} W Ω/K^2) is close to that for in-plane HOPG (2.9×10^{-6} W Ω/K^2) and is below that for through-thickness HOPG (5.4×10^{-5} W Ω/K^2). This supports the notion that the a-axis conduction path predominates the through-thickness conduction of exfoliated graphite compacts.

The Lorentz number (7.3×10^{-6} W Ω/K^2) in the through-thickness direction is comparable to the values for flexible graphite in the in-plane direction (5.6×10^{-6} W Ω/K^2 [9]). The degree of preferred orientation, which varies with the density, has little effect, if any, on the Lorentz number in both the through-thickness direction (this work) and the in-plane direction [9]. The Lorentz number of exfoliated graphite compacts is close to that of polycrystalline graphite (AXF-5Q, Poco Graphite, Inc., 4.7×10^{-6} W Ω/K^2). These observations support the predominance of the a-axis conduction path in the through-thickness conduction and furthermore mean that phonons govern the thermal conduction to similar degrees for various degree of preferred orientation.

The through-thickness thermal conductivity of the compact decreases with increasing density. This trend agrees with that reported in Ref. [9,10], but is opposite to that in Ref. [16], which reports that this conductivity increases with increasing density. As for the thermal conductivity of the compact, the thermal conductivity of the solid (graphite) part of the compact decreases [from 550 to 21 W/(m K) for the Hashin–Shtrikman model and from 370 to 16 W/(m K) for the Rule of Mixtures] with increasing density. The variation of the thermal conductivity upon change in density is more significant than that of the thermal conductivity of the overall compact (only from 8 to 5 W/(m K)).

The through-thickness electrical conductivity of the compact decreases with increasing density. This trend is opposite to that in Ref. [14,15], which report that this conductivity increases with increasing density. The incorrect opposite trend [14,15] is attributed to the unreliable two-probe method used in the conductivity measurement [14,15]. As for the overall compact, the electrical conductivity of the solid (graphite) part of the compact decreases (from 230 to 10 kS/m for the Hashin–Shtrikman model and from 150 to 7 kS/m for the Rule of Mixtures) with increasing density. The variation of the electrical conductivity upon change in density is more significant than that of the conductivity of the overall compact (only from 3.21 to 2.12 kS/m).

Corrosion resistant and high-temperature resistant sheets that are thermally and electrically conductive in the through-thickness direction are needed for the bipolar plates of fuel cells and flow batteries. At the low solid content of 2–7 vol.%, the exfoliated graphite compact exhibits electrical conductivity (2.8–3.2 kS/m for the overall compact, compared to 100 kS/m for the industrial target [11]) and thermal conductivity {7.0–7.7 W/(m K) for the overall compact, compared to 10 W/(m K) for the industrial target [11]} in the through-thickness direction. However, the thermal and electrical conductivities of the solid part of the compact is up to 550 W/(m K) and 230 kS/m respectively.

REFERENCES

[1] Chung DDL. Exfoliation of graphite. J Mater Sci 1987;22(12):4190–8.
[2] Chung DDL. Graphite. J Mater Sci 2002;37(8):1475–89.
[3] Inagaki M, Kang F, Toyoda M. Exfoliation of graphite via intercalation compounds. Chem Phys Carbon 2004;29:1–69.
[4] Celzard A, Mareche JF, Furdin G. Modelling of exfoliated graphite. Prog Mater Sci 2005;50(1):93–179.
[5] Ionov SG, Avdeev VV, Kuvshinnikov SV, Pavlova EP. Physical and chemical properties of flexible graphite foils. Mol Cryst Liq Cryst Sci Technol A 2000;340:349–54.
[6] Chung DDL. Flexible graphite for gasketing, adsorption, electromagnetic interference shielding, vibration damping,

electrochemical applications, and stress sensing. J Mater Eng Perform 2000;9(2):161–3.
[7] Chen P, Chung DDL. Viscoelastic behavior of the cell wall of exfoliated graphite. Carbon 2013;61:305–12.
[8] Chung DDL. Interface-derived extraordinary viscous behavior of exfoliated graphite. Carbon 2014;68:646–52.
[9] Wei XH, Liu L, Zhang JX, Shi JL, Guo QG. Mechanical, electrical, thermal performances and structure characteristics of flexible graphite sheets. J Mater Sci 2010;45:2449–55.
[10] Gallego NC, Klett JW. Carbon foams for thermal management. Carbon 2003;41:1461–6.
[11] Cunningham BD, Huang J, Baird DG. Review of materials and processing methods used in the production of bipolar plates for fuel cells. Int Mater Rev 2007;52(1):1–13.
[12] Bonnissel M, Luo L, Tondeur D. Compacted exfoliated natural graphite as heat conduction medium. Carbon 2001;39:2151–61.
[13] Py X, Olives R, Mauran S. Paraffin-porous-graphite-matrix composite as a high and constant power thermal storage material. Int J Heat Mass Transfer 2001;44:2727–37.
[14] Fu Y, Hou M, Liang D, Yan X, Fu Y, Shao Z, et al. The electrical resistance of flexible graphite as flowfield plate in proton exchange membrane fuel cells. Carbon 2008;46:19–23.
[15] Qian P, Zhang H, Chen J, Wen Y, Luo Q, Liu Z, et al. A novel electrode-bipolar plate assembly for vanadium redox flow battery applications. J Power Sources 2008;175:613–20.
[16] Lu Hsin-Fang, Kuo Wen-Shyong, Ko Tse-Hao. On the microstructures and thermal conductivities of exfoliated graphite. In: SAMPE Conference Proceedings, vol. 51; 2006. p. 48/1–8.
[17] Han S, Chung DDL. Increasing the through-thickness thermal conductivity of carbon fiber polymer-matrix composite by curing pressure increase and filler incorporation. Compos Sci Technol 2011;71(16):1944–52.
[18] Hashin Z, Shtrikman S. A variational approach to the elastic behavior of multiphase minerals. J Mech Phys Solids 1963;11(2):127–40.
[19] Sun K, Stroscio MA, Dutta M. Graphite c-axis thermal conductivity. Superlattices Microstruct 2009;45(2):60–4.
[20] Lindsay L, Broido DA, Mingo N. Flexural phonons and thermal transport in multilayer graphene and graphite. Phys Rev B 2011;83:235428.
[21] Efimov V, Mezhov-Deglin L. Phonon-defect interaction in carbon samples of different allotropic modifications. Phys Status Solidi C 2004;1(11):2987–90.
[22] Klemens PG. Theory of the a-plane thermal conductivity of graphite. J Wide Bandgap Mater 2000;7(4):332–9.
[23] Callister Jr WD, Rethwisch DG. Fundamentals of materials science and engineering. 4th ed. Wiley; 2012. Appendix B.
[24] Powell RW. The thermal and electrical conductivities of a sample of Acheson graphite from 0°C to 800°C. Proc Phys Soc 1937;49:419–25.
[25] Hedge SG, Lerner E, Daunt JD. Thermal and electrical conductivity of exfoliated graphite at low temperatures. Cryogenics 1973;13(4):230–1.